DESIGN AND PERFORMANCE EVALUATION OF A TOBACCO-CLIP LOADING AND UNLOADING DEVICE FOR BULK-CURING BARNS

/

密集烤房烟夹装卸装置设计及性能试验

Qingqing LÜ[1)], Yunlan MAO[1)], Ruixue LIU[1)], Kun ZHAO[1)], Xiaodong LIU[1)], Guangxi LI[1)], Liquan YANG[1,2*)], Guangyu YIN[2*)]

[1)] Henan Province Engineering Research Centre of Ultrasonic Technology Application, Pingdingshan University, Pingdingshan 467000, China;

[2)] Pingdingshan Company, Henan Tobacco Company, Pingdingshan 467033, China;

** Corresponding author: Liquan YANG, Guangyu YIN*

Tel: +8618339975718; E-mail: 2695@pdsu.edu.cn, 17703758110@163.com

DOI: https://doi.org/10.35633/inmateh-79-48

***Keywords:** tobacco bulk-curing barn; tobacco-leaf loading and unloading; semi-automatic auxiliary platform; scissor-lift mechanism; belt-scale control*

ABSTRACT

To address the high labour intensity, low operating efficiency, and safety risks associated with loading and unloading flue-cured tobacco leaves in bulk-curing barns, a tobacco-clip loading and unloading device suitable for the confined barn environment was developed. The device integrates a powered platform, a two-stage scissor-lift mechanism, and an online weighing and conveying system. Mechanical modeling and finite element analysis were conducted to verify the structural strength and overturning stability of the lifting mechanism under a rated load of 350 kg and a maximum lifting height of 3 m. The resulting overturning stability coefficient was approximately 2.9. Within an inclination range of 0°–25°, the mass-measurement error of the conveying system did not exceed 0.40%. Field performance tests showed that the maximum conveying rate reached one tobacco clip every 2.7 s. The loading time for a single bulk-curing barn was reduced from 4 h to 1.5 h, while the required labour force decreased from four workers to two. Overall operating efficiency increased by 4.33 times, and the mean time between failures met the requirements for continuous operation during the tobacco-curing season. The developed device enables efficient, low-cost, and reliable loading and unloading of flue-cured tobacco leaves and provides technical support for improving the quality and efficiency of flue-cured tobacco production.

摘要

针对密集烤房烟叶装卸作业中存在的劳动强度大、作业效率低、安全隐患突出等问题，研究设计了一种适配密集烤房环境的烤房烟夹装卸装置。该装置集成了动力平台、二级剪叉式升降机构、在线称重输送系统，以适应烤房狭小空间。通过力学建模与有限元分析，验证了升降装置在额定载荷 350 kg、最大升降高度 3 m 条件下的结构强度与抗倾覆稳定性，抗倾覆系数 K≈2.9；输送系统在 0°–25°倾斜范围内的质量检测误差率不超过 0.40%；现场性能测试表明，装置单夹运输时间最短为 2.7 s，每烤房装烟时间由人工的 4 小时缩短至 1.5 小时，用工由 4 人减少至 2 人，作业效率提升了 4.33 倍，平均无故障运行时间满足烤烟季连续作业要求。该装置实现了烟叶装卸的高效低成本与高可靠性，为烤烟生产的提质增效提供了技术支撑。

INTRODUCTION

China is one of the world's major producers of flue-cured tobacco, and most of the crop is now cured in bulk-curing barns *(Liu, 2024)*. Over the past two decades, field operations from transplanting to stalk removal have become increasingly mechanized; however, tobacco loading and unloading are still performed manually. High labour costs, heavy workloads, and a low level of operational standardization remain the main challenges at this stage. Together, these constraints have hindered the tobacco industry's transition toward more efficient, large-scale, and intensive production.

Curing quality depends on two things: how the fans and heat exchangers hold airflow, temperature and humidity, and how the sticks are stacked on the racks (*Liang et al., 2014*). The heat side has moved faster. Ge et al. optimised a tobacco-drying heat pump that recovers waste heat from a nearby data centre, cutting the primary energy input while keeping drying temperatures within target (*Ge et al., 2024*). Wang et al. took a related route, integrating dehumidification into an air-source heat pump and reporting an average COP of 2.85 across a full curing cycle (*Wang et al., 2025*).

Both gains assume that the sticks are already stacked evenly and that the load per rack is known. Neither condition can be checked by the barn operator in the field today.

Zhang built a toppling-rotary rig that swings sticks from a horizontal frame onto the vertical racks (*Zhang, 2023*), and Jiao followed with an inclination stage that lets the loaded rack tilt into position (*Jiao, 2025*). *Lin et al*. and *Ai et al*. took a different route, using a side-mounted chain to hoist the sticks along the barn wall, which gives a smaller footprint and lower peak power (*Ai et al., 2025; Lin et al., 2021*). What none of these prototypes offers is a lift geometry sized to the door and rack layout of a Chinese curing barn, or an on-line record of the weight loaded onto each rack.

Guo et al. reported a mast-lift loading machine for dense curing barns, raising sticks to 1.3–3.6 m and tilting them by 0–32° through staggered linear modules; field trials returned a loading success rate above 90% at 2.89–4.60 times the throughput of manual work (*Guo et al., 2026*). However, this prototype does not record the weight loaded onto each rack, nor is it sized as a station platform placed at the barn door. These are the two functions that determine whether uneven rack loading can be detected before firing begins.

Islam et al. used a bond-graph model to predict the dynamic response of a scissor lift under load (*Islam et al., 2014*). Their study did not extend to static structural strength or anti-tipping stability under an off-centre agricultural payload. These are the conditions a barn-door platform must survive when a fully loaded rack is lifted to 3 m. For on-line weighing during the handling cycle, *Cveticanin, (2003),* proposed a walking-speed model that keeps the weighing error low while the payload moves on a horizontal belt. The accuracy of that approach on a tilted belt has not been reported. The present work addresses both gaps: FEA-based static and anti-tipping verification and belt-scale calibration over a 0^{o}-25^{o} tilt range.

This study designs and tests a loading and unloading device for cured tobacco, sized to the operating conditions inside a dense curing barn. The working environment and the load requirements were analysed first, and the overall layout of the power platform, the two-stage scissor lift, the conveying system and the control unit was drawn up on that basis. The strength and stability of the key parts were then checked by mechanical calculations and finite element analysis. A prototype was built and taken to a working barn, where its efficiency, safety and reliability were measured. The goal is a compact and easy-to-operate machine that lowers the physical load on operators, raises loading throughput, and supports the mechanisation and large-scale operation of tobacco curing.

MATERIALS AND METHODS

Overall structural design of the loading and unloading device for tobacco clips

The loading and unloading device for tobacco clips comprises a power platform, lifting device, conveying system, and control system. The power platform includes a power system and walking mechanism (*Li and Kang, 2020*). The walking mechanism adopts a four-wheel-drive design and is driven by an electrically remote-controlled chassis. The lifting device is a core component of the system. It uses a compact and highly load-resistant two-stage scissor-type lifting mechanism, which is driven by a hydraulic system to adapt to the maximum height of the tobacco rack in the curing barn. The conveying platform adopts a chain roller-driven conveyor belt structure with an adjustable inclination to improve conveying efficiency. The control system integrates weighing sensors, speed sensors, and proximity switches to achieve automatic control. The overall structure of the device is shown in Figure 1, and the main parameters are listed in Table 1.

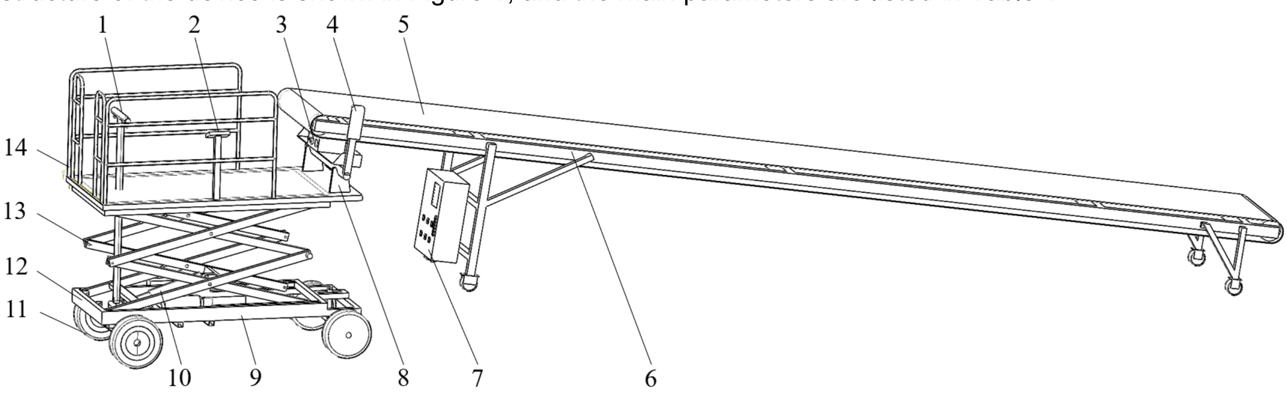

Fig. 1 - Structure diagram of the loading and unloading device for tobacco racks in the curing barn

(1) Steering handle; (2) Remote control panel; (3) Start button; (4) Proximity switch; (5) Conveyor belt; (6) Truss-type steel structure frame; (7) Control cabinet; (8) Front fork; (9) Remote-controlled electric chassis; (10) Hydraulic cylinder; (11) Walking wheels; (12) Battery box; (13) Scissor mechanism; (14) Fence

Table 1

Main Parameters of the Tobacco-Rack Loading and Unloading Device

Parameter	Value
Overall dimensions [mm]	8000×1000×3000
Rated platform load [kg]	350
Rated conveyor load [kg]	150
Power supply [V]	AC 220, DC 48
Power [W]	AC 375, DC 1000
Belt speed [m/min]	22
Adjustable inclination angle [°]	0–25
Number of operators	2

Design of the Lifting Device

Overall design of the lifting device

As the core component of the device, the lifting mechanism directly determines the efficiency and safety of the loading and unloading process. The scissor mechanism is the core component of the lifting device, and its design parameters affect the lifting performance (*Paramasivam et al., 2021*). *Huy et al. (2022)* used the MARCOS multi-criteria decision-making method to optimise the choice of scissor mechanism. Following their approach, and taking the working conditions and design requirements into account, a two-stage scissor mechanism was adopted here.

The structure is illustrated in Figure 2.

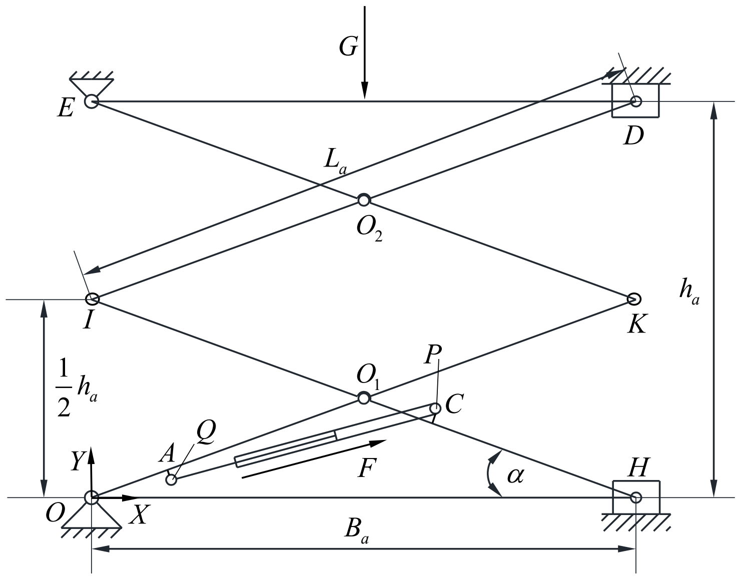

Fig. 2 - Schematic of the scissor-lift mechanism

As shown in Figure 2, O is the origin of the lifting structure coordinate system, DE is the worktable, AC is the lifting hydraulic cylinder, and B_a is the distance between O and H. EK, KO, DI, and IH are the scissor arms; L_a is the length of the scissor arm; O_1O, O_1H, O_1K, O_1I, O_2I, O_2K, O_2D, and O_2E have the same length; P and Q are the connection points between the upper and lower ends of the lifting hydraulic cylinder and scissor arms; O is the hinge point between the scissor arm and frame; E is the hinge point between the scissor arm and worktable; O_1 and O_2 are the hinge points of the two scissor arms; h_a is the lifting height of the worktable; G is the total weight of the worktable and load; α is the angle between the scissor arm and horizontal plane; and F is the thrust of the lifting hydraulic cylinder (*Yu, 2021*).

Optimisation of the hydraulic cylinder therefore focused on three factors: the maximum load, the stroke, and the movement speed. The force conditions of the scissors-lifting mechanism during the lifting process are illustrated in Figure 3.

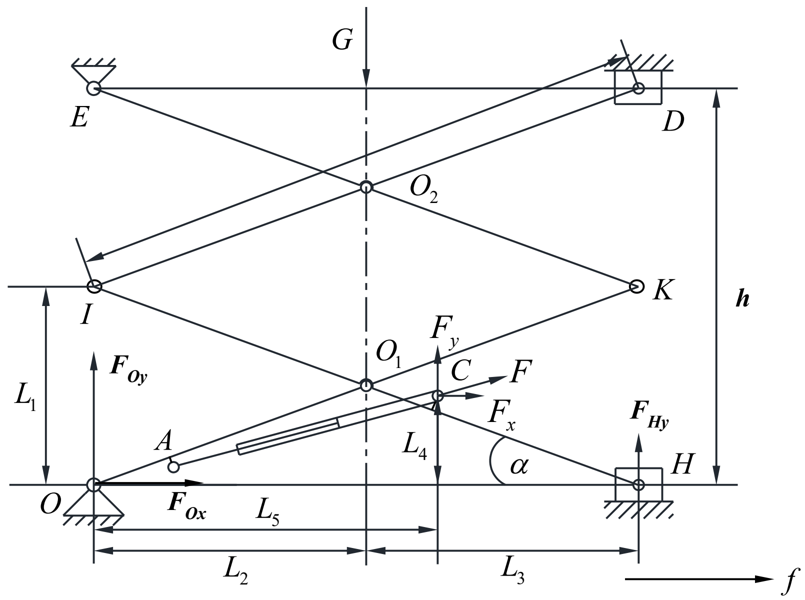

Fig. 3 - Force analysis of the scissor-lift mechanism

As shown in Figure 3, F_{Ox} and F_{Oy} are the horizontal and vertical restraining forces of the fixed hinge support O point on the mechanism, respectively; F_x and F_y are the horizontal and vertical components of the hydraulic cylinder thrust F, respectively; F_{Hy} is the vertical supporting force of the sliding hinge support H on the mechanism; f is the sliding friction force generated between the sliding hinge support H and the guide rail; L_1 is the vertical distance from the fixed hinge support O point to the hinge point I; L_2 is the horizontal distance from the fixed hinge support O point to the symmetry centre line of the mechanism; L_3 is the horizontal distance from the sliding hinge support H to the symmetry centre line of the mechanism; L_4 is the vertical distance from the force point C of the hydraulic cylinder to OH; and L_5 is the horizontal distance from the fixed hinge support O point to the force point C of the hydraulic cylinder. According to Figure 3, the equilibrium equation is listed as follows:

$$F_x = F\cos\alpha \tag{1}$$

$$F_y = F\sin\alpha \tag{2}$$

$$F_{O_x} + F_x + f = 0 \tag{3}$$

$$F_{O_y} + F_{H_y} + F_y - G = 0 \tag{4}$$

$$f = F_{H_y} \times \mu \tag{5}$$

At point O, list the torque equilibrium equation

$$G \cdot L_2 + F_{H_y} \cdot (L_2 + L_1) + F_x \cdot L_4 + F_y \cdot L_5 = 0 \tag{6}$$

It is assumed that the hydraulic cylinder drives the scissor-lifting mechanism at a constant speed under the thrust force. The vertical height at which the centre of mass rises per unit time is h, the vertical distances moved by the two ends of the hydraulic cylinder are h_1 and h_2, and the distance moved at point H is s. According to the law of conservation of energy:

$$F \cdot h_1 + F_1 \cdot h_2 = G \cdot h + f \cdot s \tag{7}$$

$$F + F_1 = 0 \tag{8}$$

From Eq. (7) and (8),

$$F = \frac{G \cdot h + f \cdot s}{h_1 - h_2} \tag{9}$$

The above analysis determines the quantitative relationship between the thrust, external load, and frictional resistance of the hydraulic cylinder and the vertical displacement of the hydraulic cylinder. This inclined-cylinder layout gives good space use, a reliable structure and a compact arrangement, and was therefore adopted (*Liu, 2022*).

The lifting device is composed of a scissor arm assembly, hydraulic cylinders, guiding mechanism, platform frame, and limit switches, and can achieve safe and reliable lifting. Considering the working conditions of the tobacco rack in the curing barn with a height of 3.6 m, the maximum lifting height of the device was determined to be 3 m. When the machine is fully lowered, the height is 0.5 m, which meets the requirements for free movement within the curing barn. A dedicated wireless remote control (Fonda electronic power unit) provides precise control of chassis movement. The structure of the lifting device is shown in Figure 4, and the design parameters are listed in Table 2.

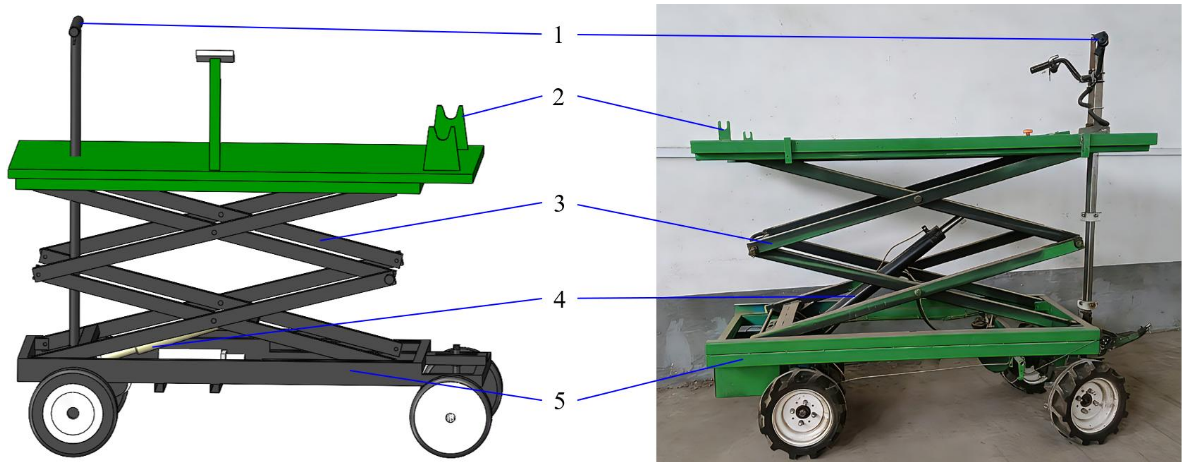

Fig. 4 - Structure of the lifting device

(1) Steering handle; (2) Front fork; (3) Scissor-lift mechanism; (4) Hydraulic cylinder; (5) Remote-controlled electric chassis

Table 2

Design Parameters of the Lifting Device

Parameter	Value
Lifting-height range [m]	0.5-3
Platform dimensions [mm]	2000×1000
Rated load [kg]	350
Lifting speed [m/s]	0.1-0.3

Design of the Hydraulic System for the lifting device

The stability of the hydraulic system is a key guarantee for the safe operation of aerial work platforms (*Liu et al., 2020*). The hydraulic system adopts a stroke-segmental speed-regulating hydraulic cylinder (Luo, 2022). The non-hydraulic end of the cylinder is equipped with two independent oil ports, and the distance between the two oil ports matches the length of the piston-sealing section. This design provides a structural basis for the regulation of segmental speed. The basic configuration of the circuit is illustrated in Figure 5.

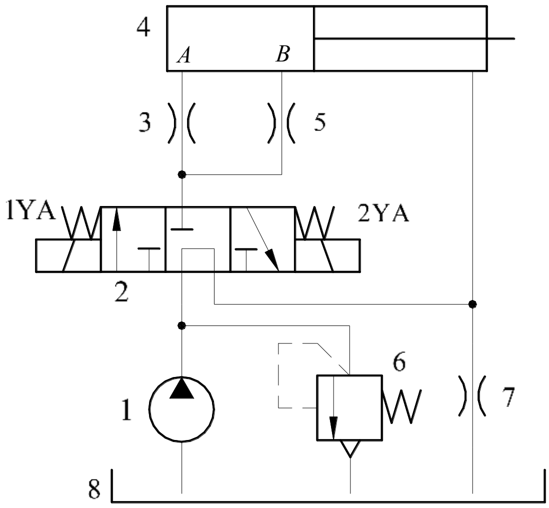

Fig. 5 - Schematic of the basic hydraulic system

(1) hydraulic pump; (2) 3-position 3-way solenoid-operated directional control valve; (3) throttle valve; (4) hydraulic cylinder; (5) flow-control valve; (6) pressure-relief valve; (7) return-line throttle valve; (8) hydraulic oil tank

During the lifting stage of the workbench, after 1YA is energised, the hydraulic pump starts to operate, and the main directional control valve switches to the left position. The high-pressure oil is sent to the left chamber of the hydraulic cylinder through throttle valve 3, and the piston rod is moved to the right. When the piston is between points A and B, the piston rod moves at a lower velocity. After the piston rod passes point B, it accelerates and reduces the lifting time of the work platform.

During the descent stage of the work platform, when the 2YA is energised, the main reversing valve switches to the right position. Under the influence of the self-weight of the scissor mechanism, the hydraulic cylinder gradually retracts. The oil in the non-hydraulic cylinder chamber flows synchronously through throttle valves 3 and 5 in both directions and exits the chamber. The scissor-lifting platform then descends rapidly to the ground. When the piston moves to the left and passes point B, the movement speed of the hydraulic cylinder decreases. The scissor-lifting platform then falls back to the initial position at a lower speed, reducing the impact and ensuring smooth descent (*Yu et al., 2021*).

Analysis of the force on the lifting device

The centre of gravity of the lifting device directly determines the stability of the lifting process. Inside the narrow space of a curing barn, precise calculation and verification are needed to make sure the machine does not tip over under static or overload conditions. This analysis centres on a two-stage scissor-lift device. A Cartesian coordinate system was set up in SolidWorks. The plane containing the bottom of the scissor mechanism was taken as the reference plane, and the centre of that bottom as the origin. The centre of gravity coordinate points were obtained within the 1-3 m lifting range, as shown in Figure 6.

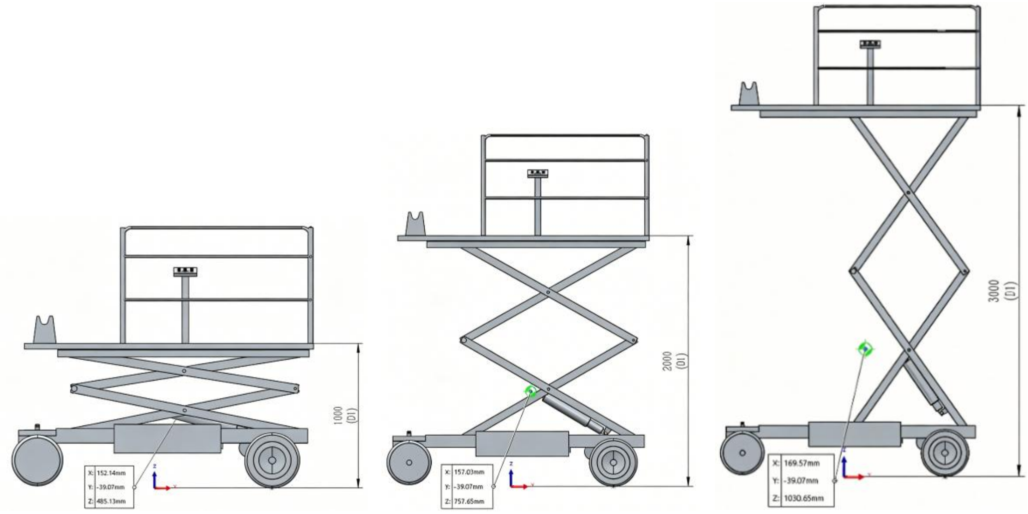

(a) Height 1000 mm *(b) Height 2000 mm* *(c) Height 3000 mm*

Fig. 6 - Point sampling process diagram

Based on the centre of gravity coordinate points, the overturning and restoring moments of the device were calculated and analysed. According to the rated load of 350 kg, the load force F = 350 × 9.8 = 3430 N. The mass of the device itself is 1046.494 kg, and its gravity G = 1046.494 × 9.8 = 10255.6412 N. The dimensions of the lifting platform are 2000 mm × 1000 mm, and the maximum lifting height is 3 m. At the maximum height, the Z-axis coordinate of the weight of the device was 1030.65 mm. The overturning moment calculation formula is shown in Eq. (10), and the restoring moment formula is presented in Eq. (11).

$$M_r = F \cdot h \tag{10}$$

where M_r is the overturning moment [N·m]; F is the load force [N]; and h is the centre of gravity height [m].

$$M_o = G \cdot d \tag{11}$$

where M_o is the restoring moment [N·m]; G is the gravity of the device [N]; and d is half the platform length.

The overturning moments at different elevations were calculated, and the results are shown in Figure 7.

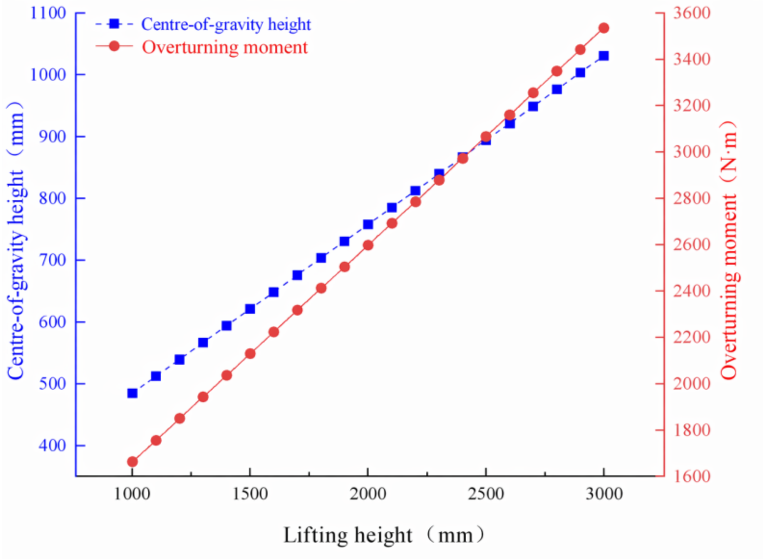

Fig. 7 - Variation in centre-of-gravity height and overturning moment with lifting height

To further verify the overturning resistance capability of the device, the overturning coefficient K was introduced as an evaluation parameter. The overturning coefficient K must be determined. According to industry standards, K should be ≥ 1.5. The overturning moment at the highest point M_r = 3430 × 1.03065 = 3535.1295 N·m, and the restoring moment M_o = 10255.6412 × 1 = 10255.6412 N·m. The overturning coefficient is calculated using Eq. (12).

$$K = \frac{M_O}{M_r} = \frac{10255.6412}{3535.1295} \approx 2.9 \tag{12}$$

The results show that under the working condition of a maximum lifting height of 3 m and a rated load of 350 kg, the restoring coefficient K is approximately 2.9, which is higher than the safety limit value of 1.5 stipulated by the industry standards. This proves that the stability of the lifting device meets the design requirements set by industry standards (*Pan et al., 2017*).

Analysis of the Load-bearing Capacity of the Lifting Device

Finite element analysis is used to verify the structural strength and stiffness of scissor mechanisms. *Dengiz et al.* obtained key parameters such as the stress distribution, deformation, and safety factor of the scissor mechanism through a SolidWorks simulation (*Dengiz et al., 2018*). Ugwuoke et al. analysed the mechanical responses of each connection point of a scissor platform using CAD simulation (*Ugwuoke and Olushola, 2023*). In this study, ANSYS Workbench was used to conduct a static analysis of the lifting device, and in accordance with the usage requirement of the platform to carry out work by two people, to ensure a sufficient safety margin, a uniformly distributed load of approximately 350 kg was applied on the working platform, which is equivalent to the load condition of four adults. A process diagram is shown in Figure 8.

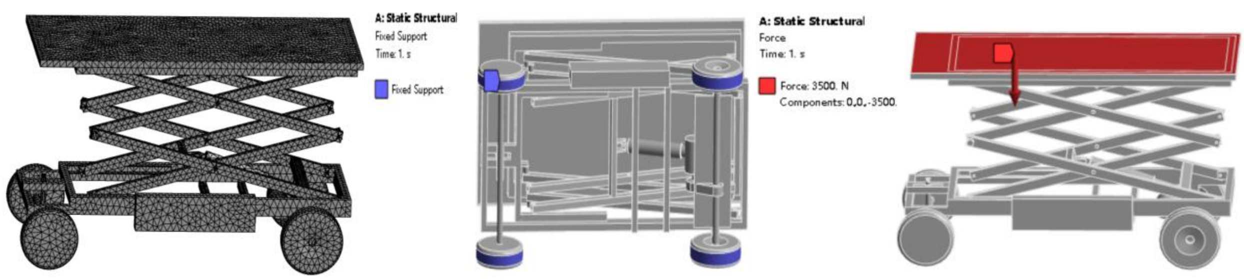

(a) Mesh generation *(b) Application of constraints* *(c) Application of the load*

Fig. 8 – Finite element analysis procedure

The finite element analysis results for the lifting device are presented in Figure 9.

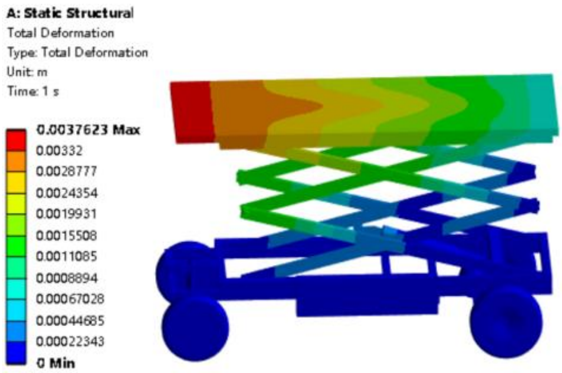

(a) Displacement cloud map

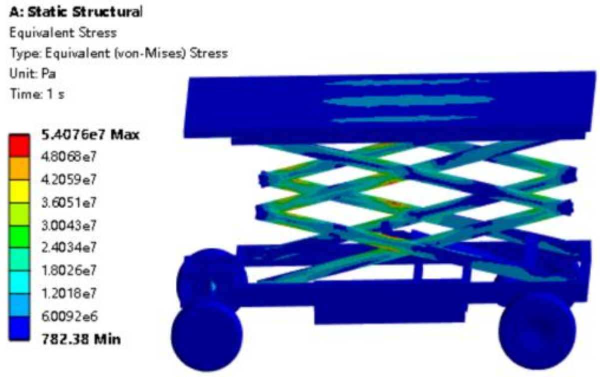

(b) Stress contour map

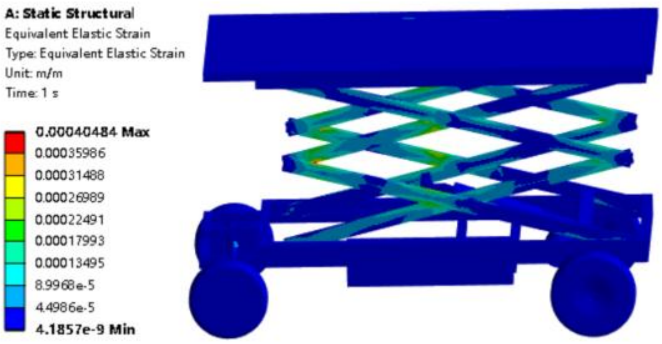

(c) Strain map

Fig. 9 - Lifting device stress contour plot

Figure 9 shows the displacement, stress distribution, and equivalent elastic strain of the lifting device under the rated load condition. The displacement distribution indicates that the platform frame has the maximum vertical downward displacement at the leftmost position, with a value of 3.7623 mm. This displacement is within the allowable engineering range and does not affect the normal operation of the equipment. The stress distribution shows that the stress concentration of the scissor mechanism mainly occurs at the movable hinge, with a maximum stress value of 54.076 MPa, which is less than the yield strength of the material and meets the strength requirements (*Shang et al., 2024; Zhao et al., 2022*). The finite element analysis results show that the scissor mechanism has good structural performance under the rated load, which is consistent with previous research results (*Bembenek et al., 2026; Ogbemhe et al., 2024*).

RESULTS

Design and Testing of Conveying Device

Overall Design of the Conveying Device

The conveying device is the core component of the tobacco clip loading and unloading system in a curing barn. It adopts a wear-resistant and anti-slip rubber conveyor belt, a high-strength and lightweight truss steel structure, an elastic adjustment device with a monitoring function (*Li, 2025*), and a control system with monitoring capabilities (*Ming and Qin, 2026*). Through the rotation of the rollers, the tobacco clips are directly borne and moved, achieving the continuous and automated conveying of the tobacco clips (*Tian, 2020*). The structural form of the conveying device is shown in Figure 10, and the design parameters are listed in Table 3.

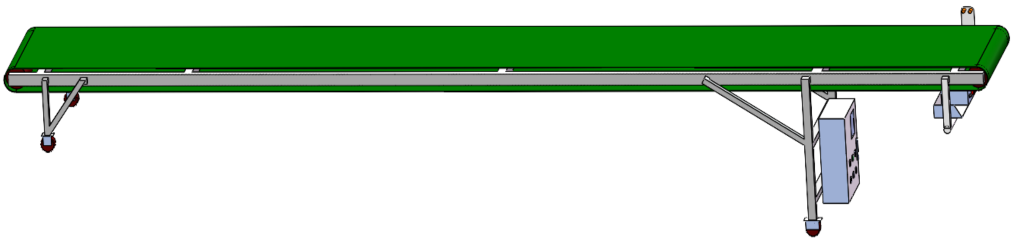

Fig. 10 - Conveyor structure

Table 3

Design parameters of the conveying device

Parameter	Value
Conveyor-belt width [mm]	920
Conveyor-belt length [mm]	7000
Conveying speed [m/min]	22
Maximum load capacity [kg]	150

Quality of Conveying Device - Correlation Test of Inclination Angle

The conveying device is prone to exhibit various tilt postures during actual operation in a curing barn. The tilt angle directly affects the quality detection accuracy and measurement stability of the belt scale. To quantify the correlation between the angle and detection quality and to optimise the system calibration parameters to ensure the reliability of the weighing data throughout the entire process, it is necessary to conduct a test on the correlation between the quality of the conveying device and tilt angle. The on-line weighing of the conveyor belt used the PSD-X3U model of the PUSHTON high-precision weighing sensor with a range of 50 kg, as shown in Figure 11.

Fig. 11 - High-precision weighing sensor

The test was conducted on the loading and unloading devices in the curing barn. The angle adjustment component and lifting device were used to achieve inclination angle regulation with an accuracy of ±0.5°. Four standard weights (5, 10, 15, and 20 kg) were used for the test. The independent variable of the test was the inclination angle of the conveyor belt, with six gradients set at 0° (horizontal reference group), 5°, 10°, 15°, 20°, and 25°, covering the travel range of the lifting device. The dependent variables were the detected mass values and detection error rates of the belt scale. The control variables included the standard weights of the conveyor belt, and running speed of the conveyor belt to ensure the reliability of the results.

Before the test, the conveyor belt was set to a 0° horizontal position and the belt scale was calibrated. The detection error should be within ±1% in the horizontal state. During the formal test, the target angle was adjusted and stabilised for 3 min. Different specifications of standard weights were placed steadily at the centre of the conveyor belt, and the conveyor belt was then started. The data were recorded after the weights completely passed through the detection zone. Each combination of angle and weight was tested three times and reset to avoid cumulative errors. The relationship between the conveyor belt inclination angle and the error rate of quality detection is shown in Figure 12.

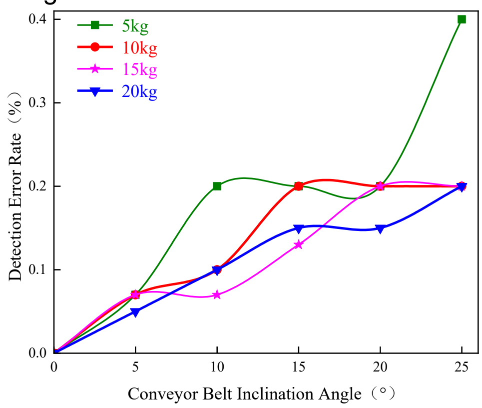

Fig. 12 - Relationship between conveyor belt inclination angle and detection error rate for different standard weights

The detection error rate rose with the belt inclination, showing a positive correlation. Under the horizontal reference state of 0°, the detection error rate for each standard weight was 0.00%. This verified the accuracy of the equipment calibration before the test and complied with the design specifications. As the inclination angle increased from 5° to 25°, the detection error rate for each standard weight gradually increased. Among them, the error rate of the 5 kg standard weight reached a maximum value of 0.40% at 25°, and the error rates of the other weights were controlled within 0.20%.

Design of the Device Control System

Considering the environment of the curing barn and the requirements of tobacco leaf handling operations, this control system features a high-precision measurement accuracy of 0.2 level, customisable interfaces, and MODBUS bus expansion. It adopts incremental digital PID control and can adapt to complex operating conditions. The automatic lifting control is set by the touchscreen to the target height and combined with limit switches to achieve deceleration when approaching the target height, ensuring stable and reliable operation. The control panel is shown in Figure 13.

(a) Control system front panel *(b) The rear panel of the control system*

Fig. 13 - The control panel

The setting of the key parameters of the control system directly determines the measurement accuracy and the control performance. The specific configuration of each parameter is as follows: the belt speed is 22 m/min, the length of the weighing section is 1 m, the speed measurement specification is 1000 P/m, the PID proportional coefficient is 8.0%, the integration time is 0.5 s, the control cycle is 50 ms, the rated load capacity of the system is 350 kg, the overload protection threshold is 110% of the rated load capacity, the belt speed deviation threshold is ±20% of the set value, the MODBUS address can be set within the range of 1 to 255, the baud rate supports 2400, 4800, 9600, and 19200 bps options, the data bit is 8 bits, the stop bit is 1 bit, and the check bit supports no check, odd check, and even check modes.

Loading and unloading measurement control is the core function of this system, which includes two processes: loading and unloading tobacco. During loading, the tobacco clip is placed on the conveyor belt, which is then started. The controller calculates the instantaneous flow rate in real time from the weight and speed sensors. When the clip reaches the end and triggers the proximity switch, the conveyor belt stops. After manual mounting and resetting, the next cycle is initiated. After the curing process is completed, the conveyor belt runs in reverse during unloading, and the measurement system accumulates the weight of the unloaded tobacco. To improve the control accuracy and response speed and reduce the adjustment fluctuations, the system adopts an incremental PID algorithm for closed-loop control. The error calculation and output correction are completed according to the PID control algorithm formula, as shown in Eq. (13).

$$\Delta \mathrm{u}(k) = K_P\left[e(k) - e(k-1)\right] + K_i \cdot e(k) + K_d\left[e(k) - 2e(k-1) + e(k-2)\right] \tag{13}$$

where $\Delta \mathrm{u}(k)$ is the increment of the kth output, K_P is the proportional coefficient, K_i is the integration coefficient, K_d is the differential coefficient, and $e(k)$ is the kth deviation.

The corresponding PID parameter adjustment strategy, adapted from established tuning rules (*Zhou, 2026*), is as follows: when adjusting the proportional coefficient (K_P), increasing K_P can enhance the system response speed, but it may lead to overshoot if it is too large; when adjusting the integral coefficient (K_i), increasing K_i can reduce the steady-state error, but it may cause integral saturation if it is too large; when adjusting the derivative coefficient (K_d), increasing K_d can improve the system dynamic characteristics and suppress overshoot.

System calibration is crucial for ensuring measurement accuracy. Zero-point calibration is used to eliminate the drift. After the load is stable, the system automatically collects and saves the zero-point value. It must be calibrated before the first use and is usually performed once a week. Range calibration is accomplished using standard weights at 50–80% of the full range to correct the coefficient. It is calibrated before the first use and is typically performed once a month. It should be recalibrated after the key components are replaced.

Overall Performance Test

Tobacco Loading and Unloading Test

The device was manufactured, assembled and commissioned according to the above design, as shown in Figure 14. The test site was the dense curing barn of the Pingdingshan Modern Tobacco Agricultural Science Park in Li Kou Town, Jia County, Henan. The curing barn was 8 m long, 3 m wide, and 4.5 m high, which meets the general standards for dense-curing barns in China. The number of layers of the tobacco racks inside the curing barn was three, with a spacing of 1.2 m per layer, and the average length and width of the test tobacco clips were 1.5 m and 0.2 m, respectively.

Fig. 14 - Photograph of the Curing Oven Tobacco Clip Loading and Unloading Device

The basic performance tests included load capacity and positioning accuracy tests. The load test was conducted by applying 200, 300, and 350 kg loads to the lifting platforms. Under each load condition, the platform was raised to a height of 3 m and maintained for 10 min to observe any sinking or deformation of the platform. Simultaneously, 100 kg and 150 kg loads were applied to the conveying device to check whether the conveyor belt slipped or had an abnormal speed. The positioning test involved raising the platform to heights of 1, 2, and 3 m, as illustrated in Figure 15.

Fig. 15 - Experimental process

The test results show that this device can stably and efficiently complete operations such as lifting and lowering tobacco leaves, transportation, and loading into curing racks. It can adapt well to the curing barn environment and significantly improve operational efficiency.

Loading and Unloading Efficiency Test

To test the efficiency of the device for loading and unloading, a comparative test was conducted using a traditional manual method. The loading and unloading operations were performed separately in the same dense tobacco curing barn, and the operation time, number of workers, efficiency, and labour cost were recorded. The results showed that it took four hours and four workers to manually load tobacco into each curing barn. After adopting the tobacco curing barn tobacco clip loading and unloading device, the loading time for each curing barn was reduced to 1.5 h, and only two workers were needed to operate it. The comparison results indicated that the operation time was shortened from 4 h to 1.5 h, saving 62.5%; the number of workers was reduced from 4 to 2, and the labour cost decreased by 50%. The overall efficiency increased by 4.33 times.

CONCLUSIONS

This study addresses the problems in China's tobacco curing process, such as the reliance on manual operations for loading and unloading of tobacco leaves in curing barns, high labour intensity, low efficiency, and significant safety hazards. The design, analysis, manufacturing, and test verification of a loading and unloading device for tobacco leaves in curing barns were completed, and a technical solution suitable for dense curing barns was developed. The main conclusions are as follows:

(1) The device integrates a four-wheel-drive power platform, a two-stage scissor-type lifting mechanism, an on-line weighing and conveying system, and an incremental-PID control loop into a single barn-door station. The rated load is 350 kg and the lifting range is 0.5–3 m, meeting the requirements for loading tobacco in dense curing barns.

(2) A method combining mechanical modelling with finite element analysis provided a scientific basis for design verification of the scissor mechanism. Under the rated load, the maximum deformation was 3.7623 mm and the maximum stress was 54.076 MPa, both within the strength and stiffness limits. At the 3 m maximum lift and 350 kg rated load, the restoring coefficient K was approximately 2.9, well above the industry safety limit of 1.5.

(3) The conveying device adopted a truss-type steel structure with a rubber conveyor belt. Weighing tests over the 0°–25° inclination range gave a maximum error rate of ≤ 0.40 %, clarifying the influence of belt inclination on weighing accuracy and ensuring accurate weight detection across the full operating angle.

Field trials showed that the shortest transportation time per clip was 2.7 s, the loading time per curing barn was reduced from 4 h under manual operation to 1.5 h, and the number of operators was decreased from four to two, giving a 4.33-fold gain in overall efficiency. The fault-free working time met the requirements for continuous operation during the tobacco-curing season. Compared with manual loading, the device lowers labour intensity and improves the consistency of the loading and unloading process. Compared with hand loading, the device reduces manual intervention, lowers the physical demand on operators, removes the variability of hand loading, and improves the accuracy and stability of the loading and unloading process.

The main scientific contributions of this work are threefold. First, it presents a barn-door station platform that integrates power transfer, scissor lifting and on-line belt weighing into a single mobile unit, moving the loading task from inside the barn to a controlled workstation at the barn door. Second, it provides a quantitative restoring envelope for a two-stage scissor lift under an off-centre agricultural payload, with an restoring coefficient of K ≈ 2.9 at a lifting height of 3 m and a rated load of 350 kg. Third, it reports a measured error envelope of ≤ 0.40 % for on-line belt weighing across the 0°–25° tilt range, filling the gap in tilt-dependent weighing accuracy for agricultural conveyors. Together, these results supply reusable design data for the mechanised loading stage of dense-curing barns.

The field trial covered a single curing season, one site and one tobacco variety. Multi-region and multi-variety trials will be undertaken to verify adaptability across leaf moisture levels and barn geometries. The belt-scale weighing was validated only within a 0^{o}-25^{o} tilt range and under uniform loading. The model will be extended to wider tilt angles, higher loading rates and non-uniform leaf distribution. Integration with machine-vision leaf grading and IoT-based curing monitoring will also be explored to enable closed-loop optimisation of the curing chain.

ACKNOWLEDGEMENT

This research was funded by the Henan Science and Technology R&D Program Joint Fund (Industrial Category) (grant No. 202324119, 20250104); Henan Key Research and Development and Promotion Special Project (Science and Technology Tackling) (grant No. 262102231017, 262102231018, 252103810171), and Henan Province Tobacco Company Pingdingshan Company Science and Technology Project (PYKJ202204).

REFERENCES

[1] Ai, Y., Wen, Y., Sun, H., Zhou, X., Zheng, L., Zhang, F., Liu, G., Su, C., (2025). Design and experiment of chain side-lifting tobacco loading machine (链条侧举升式装烟上炕机设计与试验). *Agricultural Engineering*, Vol.*15*, no.3. Beijing/China. https://doi.org/10.19998/j.cnki.2095-1795.202503318

[2] Bembenek, M., Nurkusheva, S., Mykhailiuk, V., Deineha, R., Slabyi, O., Kowalski, Ł., Osyra, M., (2026). Lightweight Design and Safety Optimization of Scissor Lift Components Using FEM. *System Safety: Human-Technical Facility-Environment*, Vol.8, no.1, pp.58-69. Warsaw / Poland. https://doi.org/10.2478/czoto-2026-0006

[3] Cveticanin, D., (2003). New Approach to the Dynamic Weighing of Livestock. *Biosystems Engineering*, Vol.*86*, no.2, pp.247-252. Amsterdam/Netherlands. https://doi.org/10.1016/S1537-5110(03)00116-8

[4] Dengiz, C., Şenel, M., Yıldızlı, K., Koç, E., (2018). Design and Analysis of Scissor Lifting System by Using Finite Elements Method. *Universal Journal of Materials Science*, Vol.*6*, no.2, pp.58-63. San Jose/USA. https://doi.org/10.13189/ujms.2018.060202

[5] Ge, Z., Zhou, Y., Li, J., Zhang, X., Xu, J., Yang, F., (2024). Multi-objective optimization and benefit evaluation of heat pump system for tobacco drying using waste heat from data center. *Journal of Cleaner Production*, Vol.*448*, pp.141623. Amsterdam/Netherlands. https://doi.org/10.1016/j.jclepro.2024.141623

[6] Guo, T., Tang, H., Li, M., Liu, C., Chen, C., Wang, L., (2026). Design and experiment of transfer and loading machine for tobacco poles in bulk curing barn scenario. *Frontiers in Plant Science*, Vol.17 - 2026. Lausanne/Switzerland. https://doi.org/10.3389/fpls.2026.1801854

[7] Huy, T. Q., Liem, N. B., Hau, T. Q., Cuong, D. Q., Danh, T. H., Nga, N. T. T., Pi, V. N., Thieu, N. N., (2022). Application of MARCOS Method for Selecting the Best Schema of Scissors Mechanism. *Lecture Notes in Networks and Systems Advances in Engineering Research and Application (ICERA 2022)*, Vol.602, pp.234-243, Cham/Switzerland. https://doi.org/10.1007/978-3-031-22200-9_25

[8] Islam, M. T., Yin, C., Jian, S., Rolland, L., (2014). Dynamic analysis of Scissor Lift mechanism through bond graph modeling. *IEEE/ASME International Conference on Advanced Intelligent Mechatronics*, pp.1393-1399. Besançon/France. https://doi.org/10.1109/AIM.2014.6878277

[9] Jiao, T., (2025). *Design and Test of Rotary Inclined Automatic Tobacco Loader (旋转倾斜式自动装烟机设计与试验)* Master's Thesis, Northwest A&F University, Shaanxi/China. https://link.cnki.net/doi/10.27409/d.cnki.gxbnu.2025.000600

[10] Li, Q., (2025). Design of Automatic Tensioning Device for Mining Belt Conveyor (矿用带式输送机自动张紧装置设计). *Rock Drilling Machinery & Pneumatic Tools*, Vol.51, no.5, pp.48-50. Gansu/China. https://doi.org/10.19449/j.cnki.2095-6282.2025.05.016

[11] Li, W., Kang, F., (2020). Design and Analysis of Steering and Lifting Mechanisms for Forestry Vehicle Chassis. *Mathematical Problems in Engineering*, Vol.2020, no.1, pp.5971746. London/UK https://doi.org/10.1155/2020/5971746

[12] Liang, R., He, Z., Wen, J., Zhang, Y., Qiu, M., Huang, L., (2014). Study on effect of different loading tobacco leaf methods on curing in bulk curing barn (密集烤房不同装烟方式烘烤效果研究). *Guangdong Agricultural Sciences*, Vol.41, no.3, pp.33-35+40. Guangdong/China. https://doi.org/10.16768/j.issn.1004-874x.2014.03.012

[13] Lin, J., Gao, L., Lin, Y., Lin, Q., Lu, Y., (2021). Design and Experiment of Chain Lifting Type Tobacco Loading Machine (链条举升式装烟机的设计与试验). *China Southern Agricultural Machinery*, Vol.*52*, no.18, pp.72-74+104. Jiangxi/China. https://kns.cnki.net/kcms2/article/abstract?v=f9AMVDUgxC-xhxyX_2RLHnQKIrKW1A0UUl3Qfo2T1KXrgbU5KozKHQwCacgjdc2DDtEwdXVRsi34uE_z9Yjt5zqn8p6HQQSq3tjq5zLQ-JMNyb_LVCYA8MhJfUSA-97nE2t5gp_rziytURMqiyrflLqplsjWq-yOXwJqu2TM2JKNfgY8gOTwekUXIFuIipWy&uniplatform=NZKPT&language=CHS

[14] Liu, K., (2024,12-23). Sichuan Liangshan: "Golden Leaves" Spread Out a Road to Rural Revitalization, Consumption Daily (四川凉山：片片“金叶”铺就乡村振兴路). *Consumption Daily*. https://www.xfrb.com.cn/article/zx/17253189217091.html

[15] Liu, W., (2022). *Structure optimization design and stability research of caterpillar orchard working platform (履带式果园作业平台结构优化设计与稳定性研究)* Master’s Thesis, Hebei Agricultural University, Hebei/China. https://link.cnki.net/doi/10.27109/d.cnki.ghbnu.2022.000733

[16] Liu, Z., Ji, A., Zhang, L., Wang, H., Zhao, Z., (2020). Stability analysis of hydraulic system on scissor type aerial work platform (剪叉式高空作业平台上车液压系统的稳定性研究). *Journal of Mechanical & Electrical Engineering*, Vol.37, no.6, pp.600-606. Zhejiang/China. https://kns.cnki.net/kcms2/article/abstract?v=f9AMVDUgxC9uZtCkCORIKcAQqNREDpocsmJFBe-dVDkiCPPuxbErSKfUn9KDdRNgZ10-bdaZ6mp98uJlvUW1t61FazzuhFvh2zYnCo9nZFvjhnA99ZcvNHk0Ng6cXc8JrnSlXcBSKPlSqo7904GQ2tHd_-mx2E2gGR_F-bnLs-6LVC2vpexyNepyWVzlk-Lo&uniplatform=NZKPT&language=CHS

[17] Luo, N., (2022). Design and Simulation of Hydraulic System in Scissor Lifting Platform (剪叉式液压升降台速度控制方法及仿真分析). *Mechanical Engineer*, no.4, pp.88-90+93. Heilongjiang/China. https://kns.cnki.net/kcms2/article/abstract?v=f9AMVDUgxC_2YjagfGqpkC9F0_EJ-UhD9BuWyS2Bc5FpZE6htxSLkU1Hy_9auvR1yIfcN7abuhLQhLTjphWbeN6iB_0jqY4Wq94uRgmiQDAQn3TmDrE12_An9FwFzuyGz2FPV5b6JNsZdcbY62Tiam9_2HMJwwqGJmzBMGRyxIT-6XN-m2nyaJLQ9u5NtA7B&uniplatform=NZKPT&language=CHS

[18] Ming, Z., Qin, X., (2026). Design and Implementation of Intelligent Conveyor Belt Control System (智能传送带控制系统设计与实现). *Modern Manufacturing Technology and Equipment*, Vol.62, no.2, pp.210-212. Shandong/China. https://doi.org/10.16107/j.cnki.mmte.2026.0129

[19] Ogbemhe, J., Ramatsetse, B., Mpofu, K., George, O. A., (2024). Multi-Physical Modelling and Simulation of a Planar Translational Scissor Lift Mechanism for Maintenance of Rail Transmission Lines. *Procedia CIRP*, Vol.121, pp.174-179. Amsterdam/Netherlands. https://doi.org/10.1016/j.procir.2023.09.246

[20] Pan, C. S., Chiou, S. S., Kau, T.-Y., Wimer, B. M., Ning, X., Keane, P., (2017). Evaluation of postural sway and impact forces during ingress and egress of scissor lifts at elevations. *Applied Ergonomics*, Vol.65, pp.152-162. Oxford/UK. https://doi.org/10.1016/j.apergo.2017.06.009

[21] Paramasivam, V., Tilahun, S., kerebih Jembere, A., Selvaraj, S. K., (2021). Analytical investigation of hydraulic scissor lift for modular industrial plants in ethiopia. *Materials Today: Proceedings*, Vol.46,

pp.7596-7601. Amsterdam/Netherlands. https://doi.org/10.1016/j.matpr.2021.01.838

[22] Shang, H., Li, X., Zhang, C., Xu, C., Hou, Y., Jia, M., (2024). Optimization design and experiment of automatic leveling system for orchard operating platform in hilly and mountainous areas. *INMATEH - Agricultural Engineering*, Vol.73, no.2, pp.364-374. Bucharest/Romania. https://doi.org/10.35633/inmateh-73-30

[23] Tian, Y., (2020). On the Design of Simulation Control System for Tobacco Logistics Storage Conveyor Belt Device (论烟草物流仓储传送带装置模拟控制系统设计). *Hebei Agricultural Machinery*, no.4, pp.73. Hebei/China. https://doi.org/10.15989/j.cnki.hbnjzzs.2020.04.056

[24] Ugwuoke, I. C., Olushola, T. O., (2023). Development of a 120kg Load Lifting Capacity Scissor Elevator Platform. *International Journal of Engineering and Manufacturing (IJEM)*, Vol.13, no.6, pp.38-52. Hong Kong/China. https://doi.org/10.5815/ijem.2023.06.04

[25] Wang, J., Ruan, X., Li, P., Song, Y., Liu, X., Jia, L., Yang, Z., Duan, W., (2025). Integrated crew for heating and dehumidification of air-source heat pump for tobacco curing. *Scientific Reports*, Vol.15, no.1, pp.38062. London/UK. https://doi.org/10.1038/s41598-025-21816-7

[26] Yu, Y., (2021). *Design and Test of High-Position and Automatic Leveling Work Platform in Orchard (果园高位自动调平作业平台设计与试验)* Master's Thesis, Beijing Forestry University, Beijing/China. https://link.cnki.net/doi/10.26949/d.cnki.gblyu.2021.000356

[27] Yu, Y., Kang, F., Zheng, Y., Lü, H., Wang, Y., (2021). Design and simulation of the automatic-leveling high-position platform in orchards (果园高位自动调平作业平台设计及仿真). *Journal of Beijing Forestry University*, Vol.43, no.2, pp.150-159. Beijing/China. https://kns.cnki.net/kcms2/article/abstract?v=f9AMVDUgxC8AWEyHq55bU0R931yn3Gw4e9RN87RpoX3CZ6OnLukcoHdrMuTxH3qY_fC8v8OUt8DQxdVam_Jb4oEqHJtr6lgfSV4IO_cZeRwCsVCmnZ4MYvRN0iwISGyO--e2puxZAQSdovigNHF3y3k9ebAHPPkMWTTouNGcJXlpMcHSBM8j1kjn3OBzeeJ8&uniplatform=NZKPT&language=CHS

[28] Zhang, X., (2023). *Design and experiment of toppling rotary tobacco loading machine in Bulk Curing Barn (密集烤房倾倒旋转式装烟机设计与试验)* Master's Thesis, Southwest University, Chongqing/China. https://link.cnki.net/doi/10.27684/d.cnki.gxndx.2023.001903

[29] Zhao, G., Liu, Y., Ye, N., (2022). An improved fatigue accumulation damage model based on load interaction and strength degradation. *International Journal of Fatigue*, Vol.156, pp.106636. Oxford/UK. https://doi.org/10.1016/j.ijfatigue.2021.106636

[30] Zhou, W., (2026). A speed control system design based on fuzzy-PID controller (一种基于模糊-PID 控制器的调速系统设计). *Science and Technology & Innovation*, no.2, pp.88-91. Shanxi/China. https://doi.org/10.15913/j.cnki.kjycx.2026.02.024